ISTITUTO NAZIONALE DI FISICA NUCLEARE
Laboratori Nazionali di Frascati

LNF-85/12

M. Basile,..... M. Spinetti, G. Susinno, L. Votano et al.:
A LIMITED-STREAMER TUBE ELECTRON DETECTOR WITH HIGH REJECTION POWER AGAINST PIONS

Estratto da:
N.I.M. A235, p. 74 (1985)

Servizio Documentazione
dei Laboratori Nazionali di Frascati
Cas. Postale 13 - Frascati (Roma)

Nuclear Instruments and Methods in Physics Research A235 (1985) 74–84
North-Holland, Amsterdam

A LIMITED-STREAMER TUBE ELECTRON DETECTOR WITH HIGH REJECTION POWER AGAINST PIONS

M. BASILE, J. BERBIERS, G. BONVICINI, G. CARA ROMEO, L. CIFARELLI, A. CONTIN, M. CURATOLO, G. D'ALI, C. DEL PAPA, B. ESPOSITO, D. FABBRI, P. GIUSTI, T. MASSAM, F. MASSERA, R. NANIA, G. NATALE, F. PALMONARI, G. SARTORELLI, M. SPINETTI, G. SUSINNO, L. VOTANO and Z. ZICHICHI

CERN, Geneva, Switzerland
Dipartimento di Fisica dell'Università, Bologna, Italy
INFN, Laboratori Nazionali di Frascati, Italy
INFN, Sezione di Bologna, Italy

Received 30 May 1984

The problem of detecting electrons in the 0.5–4.0 GeV energy range, in the presence of a high pion background, has been studied using a new type of electromagnetic shower detector. Its structural properties and the main parameters are given, together with the basic results in terms of energy resolution and of rejection power against pion background. The optimization of this new instrument gives a pion rejection power of $\sim 6\times10^{-4}$ for energy $\gtrsim 1.2$ GeV.

1. Introduction

The shower detector described in this paper was built to detect prompt electrons in proton–proton interactions at ISR energies, in an experiment designed to look for the production of heavy flavours. A powerful way of separating out events with heavy-flavoured particles is to detect the prompt electron resulting from the weak semileptonic decay of one of the heavy particles (baryons or mesons) produced in pairs. This method was successfully used at the CERN intersecting storage rings to look for charmed particles [1], and produced the first evidence for a neutral baryon Λ_b^0 with a "b-quark" [2].

The main experimental requirement was the detection of a genuine single electron in a high background of pions. The energy of these prompt electrons resulting from the semileptonic decay of "c (b)-flavoured" particles is $\gtrsim 0.3$ ($\gtrsim 1.2$) GeV. Other constraints were a good spatial resolution, a large area to be covered (~ 11 m^2) and the possibility of a minimum energy cut at the fast-trigger level.

The choice of a digital electromagnetic calorimeter, built using arrays of plastic tubes with resistive cathodes operated in the limited-streamer mode (limited-streamer tubes, LSTs) [3] of 1×1 cm^2 cross-section, fit well the constraints given by the experiment.

A prototype shower detector 50×38 cm^2 was tested on an electron and pion beam of selectable momentum in order to study the energy response and resolution, the pion rejection power, the high rate effects and the optimum configuration for the ISR experiment.

In sect. 2 the prototype electromagnetic calorimeter, the test beam used, the working conditions and the calibration data taken will be described. Sect. 3 is dedicated to the results obtained for the calorimeter response to electrons, whereas sect. 4 will deal with the pion–electron discrimination. Finally, sect. 5 will summarize the characteristics of the final version of the electromagnetic calorimeter chosen for the ISR experiment.

2. The test apparatus

The test electromagnetic calorimeter was built using the same components as those foreseen for the large-area ISR detector, namely, the basic component was a standard LST array module. It consists of two arrays of eight tubes, 2.5 m long, located in a single gas-tight PVC jacket. Each tube, 1×1 cm^2 in cross-section, has a resistive graphite coating on the plastic walls and a 100 μm beryllium–copper wire stretched between the two ends and kept centred by suitable spacers. A fairly modest gas flow is maintained through all tubes of the module, ensuring complete regeneration of the gas mixture in about six hours. High voltage is supplied in parallel to the eight wires of one array through a limiting 10 MΩ resistance, whereas each wire has a matching 220 Ω resistor.

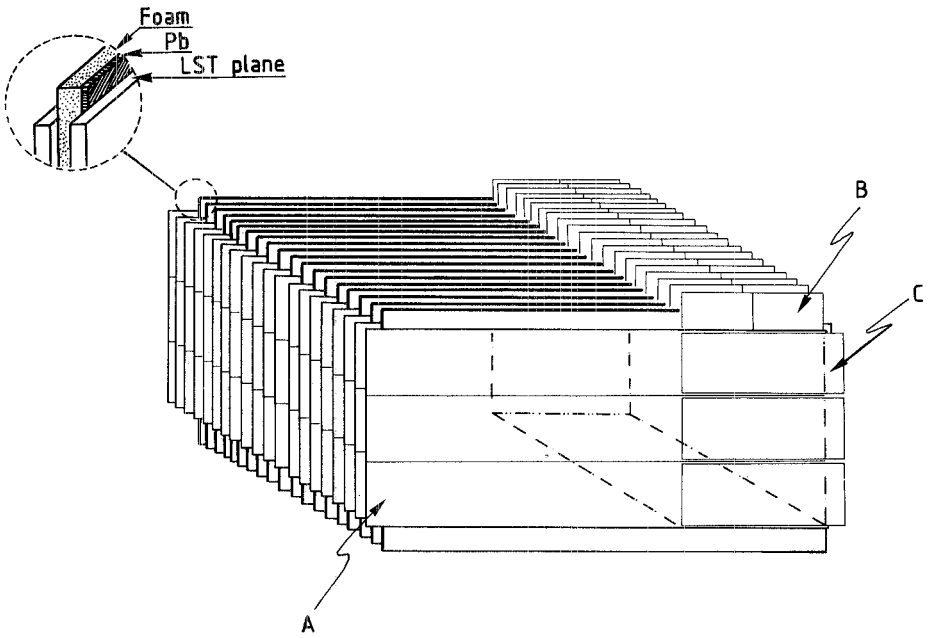

Fig. 1. The test module. (A) Planes of standard LST modules. (B) Vertical y-strips readout planes. C) Horizontal x-strip readout planes. The insert shows an expanded view of the lead absorber. The dash–dotted lines show the calorimeter fiducial volume.

The test calorimeter consisted (see fig. 1) of 19 vertical plates of lead interleaved with 20 planes of LSTs, each plane made of three LST modules, mounted side by side. To have a linear energy response up to at least 1 GeV electron energy, a 5 cm spacing was left between the lead layers. In this way an effective radiation length of about 10 cm allowed for a certain spatial development of the electron showers, as required by the 1 cm granularity of the active detector elements.

Two configurations of the lead sampling have been used in the tests, as shown in table 1.

As we will see, sampling B limited to the first 11 lead layers was finally chosen when building the ISR large-area shower detector. The first LST plane spaced in front of the first lead layer marked the position and multiplicity of the incoming beam particle(s) and was used off-line to improve the trigger by rejecting double hits or accompanying neutrals.

Each calorimeter LST plane was read out by 32 vertical y-strips (orthogonal to the wires) 50 cm long and 1 cm wide with 1.2 cm pitch, and by 48 horizontal x-strips (parallel to the wires) 0.5 cm wide with 1 cm pitch, covering only a part (38 cm) of the full LST plane length. In conclusion, the readout strips defined a sensitive area 38 cm wide by 50 cm high: the total number of strips was 1600.

Table 1
Configuration of lead sampling used in the tests

Sampling A		Sampling B	
First layer	5 mm of Pb	First layer	5 mm of Pb
Layers 2–19	3 mm of Pb	Layers 2–6	3 mm of Pb
		Layers 7–11	4 mm of Pb
		Layers 12–19	3 mm of Pb

Signals from strips (amplitude $\gtrsim 2$ mV on a 50 Ω load) were fed into a monolithic amplifier discriminator (LeCroy MIL200), giving a pulse 2 μs long. Outputs from eight contiguous channels were then fed into 8-bit, parallel-in/serial-out, shift registers. A single bus allowed serial readout of all shift registers of each plane. A single CAMAC processor (LeCroy STOS Controller 4700) was connected to eight such buses. At every trigger the processor generated the load signal to the shift registers; data were then transferred from the processors to a HP 21MX computer and written on tape.

Three parameters are relevant when setting the working conditions for the LST; gas mixture, high voltage, and threshold of the amplifier discriminator circuit.

The gas mixture determines the knee of the high-voltage plateau [3]. We used argon + isobutane in the proportion 1 : 2.2 in volume; consequently, the high-voltage plateau started at 4150 V.

The high-voltage setting determines the total charge of a streamer and therefore the amplitude of the pick-up signals. This means that there is an interplay between high voltage and discriminator threshold in determining the detection efficiency and the mean number of adjac-

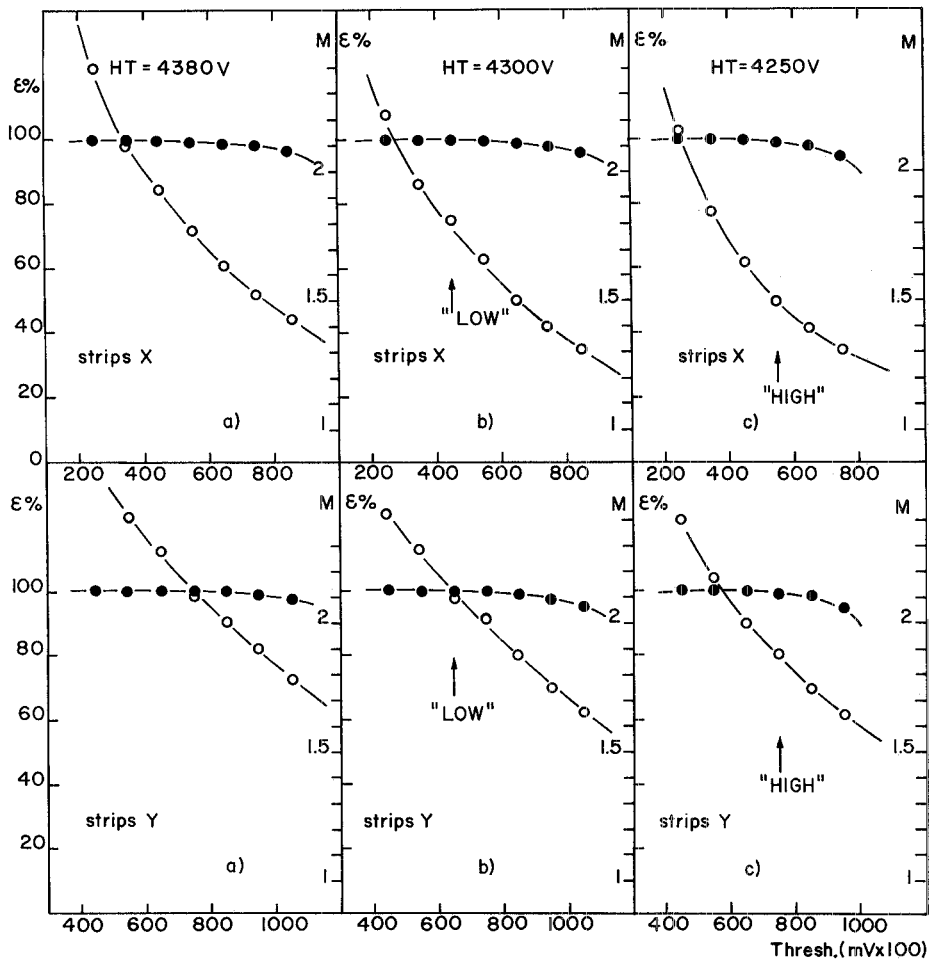

Fig. 2. Efficiency per plane ϵ (in percent), corrected for geometrical effects (full points and left scale), and mean multiplicity M per plane (open points and right scale) as a function of the hardware threshold, for three settings of the LST high voltage: (a) 4380 V, (b) 4300 V and (c) 4250 V. The gas composition was in all cases argon + isobutane in the proportion 1 : 2.2 and the high-voltage knee was at 4150 V. The arrows show the two work points chosen for the two sets of data called LOW and HIGH.

ent strip hits for a single particle crossing (i.e. the "multihit" factor M, or the mean "cluster size").

In fig. 2, for three different high-voltage settings, the single-particle efficiency and the corresponding mean number of strip signals (M value) are plotted as a function of the electronic threshold. Notice that, for purely geometrical reasons, i.e. the dead space between tubes, the maximum efficiency is of the order of 90%. As a second remark, M is approximately the same for the x- and the y-strips, the reason for this being the short length of the x-strips parallel to wires. In the final version of the calorimeter, where the strips parallel to the wires have the same length as the tubes, M is much lower, of the order of 1.2, as found in other applications of LSTs.

In figs. 2b and 2c the arrows show the two working points (called LOW and HIGH , respectively) where complete sets of pion and electron data have been collected to study the relevance of the M parameter against the calorimeter response to those particles. The values of M corresponding to the LOW and HIGH settings were respectively $M(x) = 1.8$, $M(y) = 2.1$, and $M(x) = 1.5$, $M(y) = 1.9$. We will see in sect. 3 the importance of M when studying the electron–pion discrimination.

The calorimeter, placed on a movable platform, could be centred on a momentum-selectable low-energy secondary beam of the proton synchrotron (PS) at CERN. Two plastic-scintillator counters, 10 m upstream, defined the incoming beam, and two other counters, just in front of the calorimeter, defined the beam's transverse dimensions, 3×3 cm^2. An array of scintillation counters covered the whole sensitive area of the calorimeter and acted as a veto against multiple-particle

events. Two 3 m long gas-pressurized threshold Cherenkov counters were placed upstream on the beam line and were used to select beam particle types.

The beam momentum could be selected between 500 MeV/c and 4 GeV/c, and a typical total rate figure was 3×10^3 particles per machine burst. The beam spill was flat, lasting 500 ms. The beam composition varied from around 10% of electrons at low momentum to 0.1% at 4 GeV/c, and in almost all cases, except the highest momentum settings, electron beams could be defined with less than 1% pion contamination. On the contrary, pion beams with a very low electron contamination (below 1×10^{-4}, as required to measure the pion rejection factor of the calorimeter safely) could be obtained, especially at high momenta. Another contamination of the pion beam which could affect the pion rejection factor is the muon contamination: the measured muon content, of about 0.3%, is small and does not affect the results.

We studied the effects of the total rate on the LSTs response. A simple way to evaluate the total rate seen by the test calorimeter was to measure the average current provided by the HV power supplies during the beam spill. A conservative hypothesis was to assume that this current was uniformly distributed on all the LSTs, because the low-energy particle halo of the beam was intense and very large. The resulting rate was about 10–20 Hz of streamers per centimeter of wire. Of course the corresponding number of crossing particles was lower, because interacting particles or showering electrons produced more than one streamer.

Such a rate, which is much higher than that foreseen for the ISR experiment (about 1 Hz/cm^2), did not at all affect the efficiency of the LSTs. Actually, we found no effect when comparing the responses to electrons selected at different times during the beam spill.

In conclusion, no rate effects were present in the calibration data, and this fact guaranteed a safe operation of the calorimeter in the ISR experiment, where a rate of about 10^4 particles per m^2 per second, considering beam–beam and beam–gas interactions is expected.

Data with electron and pion triggers have been collected at various beam momenta from 0.5 to 4 GeV/c in the two calorimeter configurations A and B for two settings of the LSTs high-voltage and electronic threshold. Table 2 is a summary of the collected data.

3. Calorimeter response to electrons

Typical events in the test calorimeter for electrons of 0.8, 1.5 and 3.0 GeV energy can be seen in figs. 3a, 3b and 3c, respectively. In these figures the position of x-strip and y-strip hits are displayed in the two orthogonal views, and the total number of hits is counted by the on-line analysis program. Notice that the information from the x-strips and that from the y-strips are not independent because both are induced signals, along and across the wires, of the same streamers of an LST plane. In any case, as will be seen, they are useful for separating electrons from pions because they give two orthogonal views of the shower development.

In figs. 4a–4d the longitudinal shower distribution, as measured by the calorimeter x-strips (these data refer to sampling B threshold LOW), is compared with standard shower curves for 500 MeV/c and 1.0, 2.2 and 4.0 GeV electron energy. To make this comparison, the mean number of hits in each LST plane has been divided by M. At low energy the calorimeter granularity matches the shower density so that the experimental points follow the shower curve rather well, whilst at higher energies there are increasing losses in the shower maximum.

Fig. 5 shows the total number of hits in the two views as a function of the electron energy. The upper curve refers to the full calorimeter, whilst the lower curve shows the energy response for a thinner, 12-plane calorimeter (optimized for electron–pion discrimination) , such as was chosen for the ISR experiment.

In fig. 6 the energy resolution is plotted as a function of the electron energy. In this case the upper curve refers to the 12-plane calorimeter, showing a roughly constant resolution of 20% for the ISR calorimeter, which is already adequate for performing an energy cut around 600 MeV as demanded by the experiment.

Table 2
Number of analysed events

Trigger particle	Sampling	Thresholds	Beam momentum (MeV/c)							
			500	800	1000	1200	1500	2200	3000	4000
Electron	A	LOW	3428	3893	2028	2344	4229	3687	2007	1559
Pion	A	LOW	3005	21191	5051	10108	5026	5014	5384	–
Electron	A	HIGH	–	1551	–	1546	1756	1559	2301	1497
Pion	A	HIGH	–	10102	–	10026	10012	–	12046	–
Electron	B	LOW	2575	3535	3018	3962	2504	2974	1539	3288
Pion	B	LOW	3353	25675	9036	23957	3428	3406	–	–

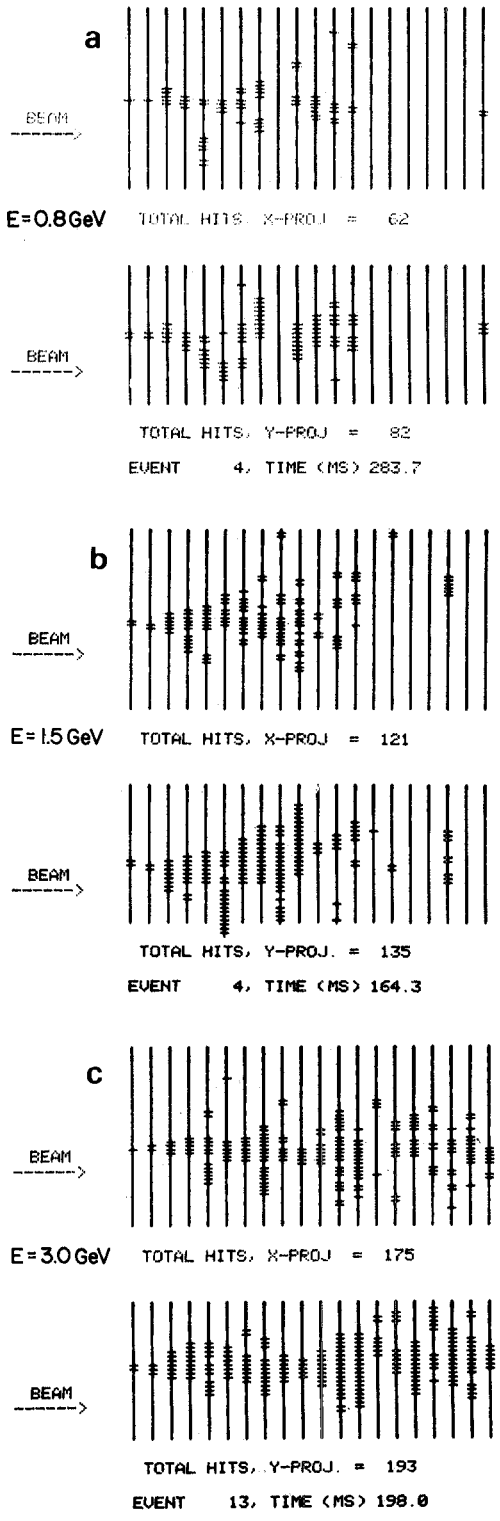

Fig. 3. Typical electron event display as shown by the on-line HP 21MX analysis program. The vertical lines represent (schematically) the 20 LST planes' readout x- and y-strips. The total number of hits per view is also indicated. Electrons of different energies are shown: (a) 0.8 GeV, (b) 1.5 GeV and (c) 3.0 GeV.

4. Pion versus electron discrimination

Using the considerable amount of pion data taken at various beam momenta (see table 2), their pattern in the LST calorimeter has been carefully studied to find the best way of distinguishing an electron from a pion.

Two typical pion events (sampling B, threshold LOW) are presented in fig. 7 for 0.8 and 1.5 GeV/c momentum pions. Here the multihit effect is clearly seen because in almost all planes the single track traversal gives two adjacent hits in x- and y-strips.

A comparison of fig. 7 (pion event display) with fig. 3 (electron event display) shows that the hit pattern is very powerful when separating pions from electrons, representing indeed a tool for reaching the ultimate rejection limit. On the other hand, the ISR experiment for which the calorimeter was envisaged requires a good pion-to-electron separation, already at the trigger level, for electrons in the range 500 to 1200 MeV.

The pion rejection obtainable with the simple cut in the total hit multiplicity was first studied for the two threshold settings, as a function of the particle energy. The cut applied corresponded to a constant electron efficiency of 90%. The result of this study is shown in fig. 8. The rejection obtainable is very good, better than 1% at 1 GeV: the LOW electronic threshold setting gives better pion–electron separation. On this basis we have chosen the LOW threshold, in spite of a loss of linearity in the energy response; all the following studies therefore refer to the above setting of the electronics. Incidentally, the upper curve in fig. 8 represents the pion rejection obtained in a lead/scintillator sandwich of comparable thickness [4]. It is interesting to note that this digitized sandwich has an order of magnitude better pion rejection, probably because of the role played by the Landau fluctuations of the energy loss, to which digital devices are less sensitive than scintillation counters.

The pion rejection obtainable with the simple hit-counting algorithm is very good but, nevertheless, not the maximum one can achieve. In fact, the whole spatial information contained in figs. 3 and 7 is compressed in one single parameter, distributed as shown in fig. 9a. To take full advantage of the rich spatial information of the digital calorimeter, many off-line pion rejection criteria have been studied using the data collected during calibration runs.

The first criterion that was found to improve the pion rejection with respect to the simple hit-counting was based on the definition of a cluster as a group N_c of adjacent strips hit simultaneously, N_c being the cluster size. Because of the M factor, a single track gives

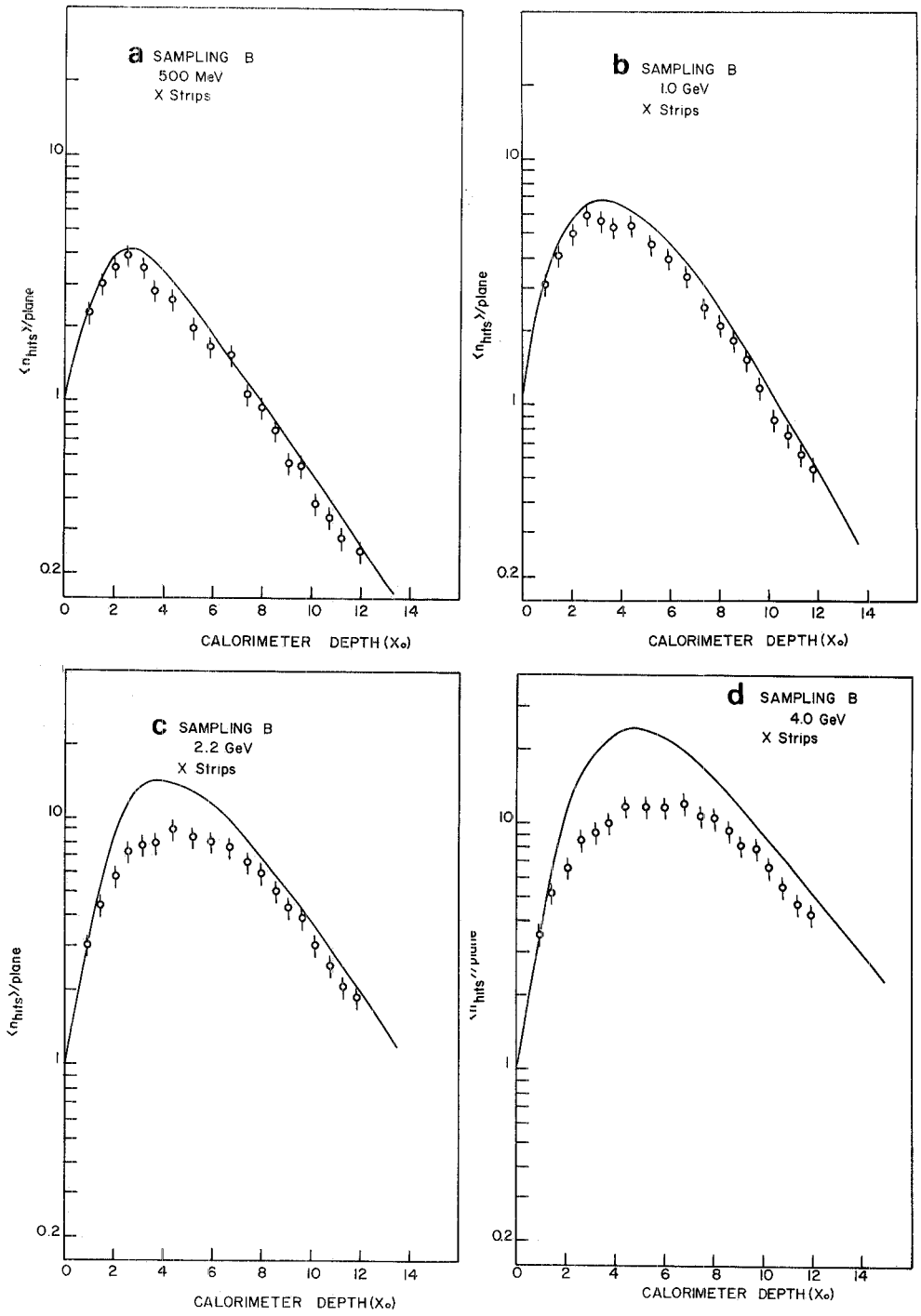

Fig. 4. Comparison between shower curves and data at four electron energies: (a) 500 MeV, (b) 1.0 GeV, (c) 2.2 GeV and (d) 4.0 GeV. The full line represents the expected mean multiplicity of electrons in the shower as a function of the depth in lead as calculated by standard electromagnetic shower curves. The experimental points are the measured mean multiplicity of hit x-strips in the 20 LST planes corrected for the M factor. The first plane, at zero depth, is not shown, being normalized at 1. The saturation effect is increasingly important at the shower maximum, whereas it is small on the tail at all energies.

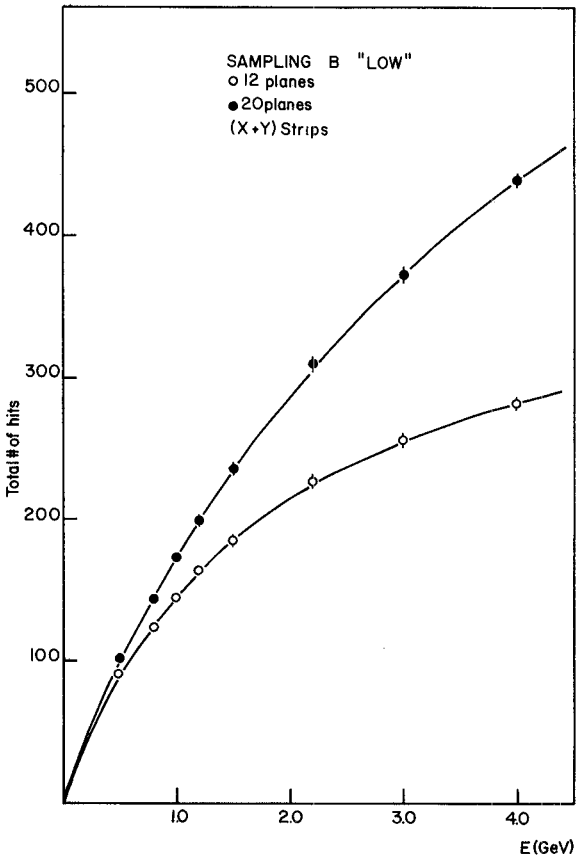

Fig. 5. Total number of x- and y-strip hits versus electron energy. The curves are hand-drawn through the data points. The upper curve refers to the full-depth calorimeter (20 planes), the lower curve to finally chosen 12-plane calorimeter.

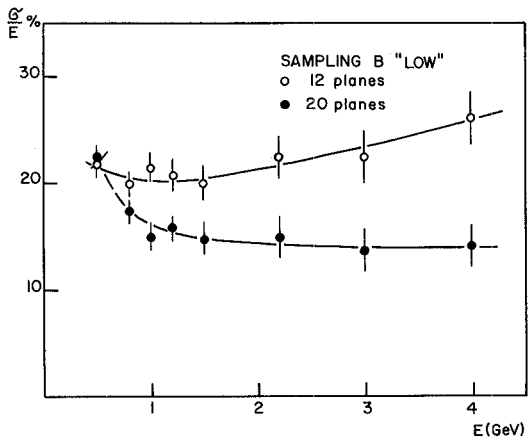

Fig. 6. Energy resolution σ/E (in percent) versus energy of electrons as found by the total number of hits in the x- and y-strips. The curves are hand-drawn through the data points. Here the lower curve refers to the full-depth calorimeter of 20 planes, the upper curve to the 12-plane one.

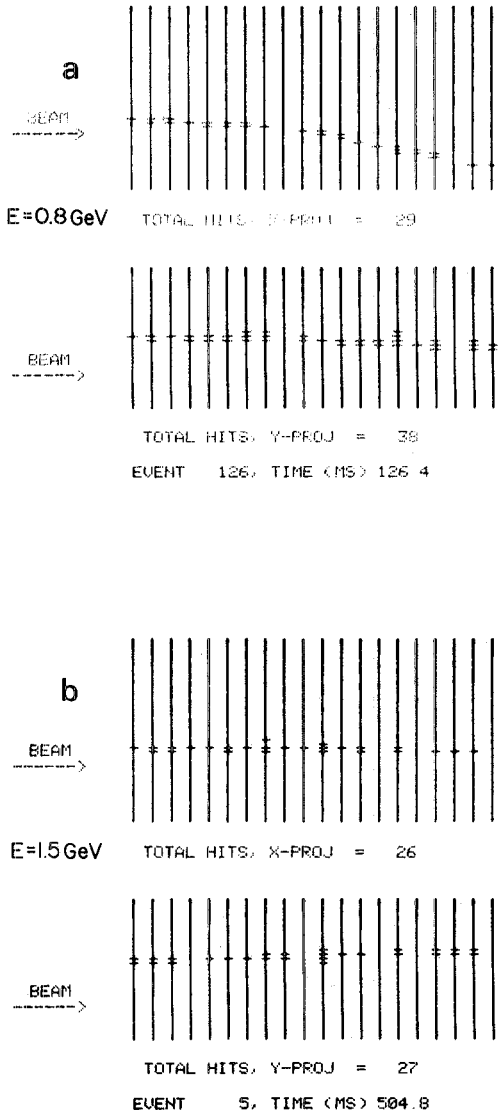

Fig. 7. Typical pion events as displayed by the on-line analysis program (cr. fig. 3). Beam momentum is (a) 0.8 GeV/c and (b) 1.5 GeV/c. Notice the small-angle nuclear scattering visible in the x-protection of event (a).

mainly size 2 clusters (see fig. 7): if one counts only clusters of size ≥ 3, the difference between pions and electrons is enhanced. This can be seen from fig. 9b, where the distribution of the hits multiplicity is shown. The arrows mark a 90% efficiency cut for electrons and show an improvement of a factor of 2 in pion rejection: the number of events left at 800 MeV/c goes from 44, corresponding to $\epsilon_\pi = 2.8‰$, to 23 events, i.e. $\epsilon_\pi = 1.5‰$.

The above combination of cuts has been used to optimize the depth of the calorimeter. The study of pion rejection has been done at 800 MeV electron energy by varying the number of LST plates added together, i.e.

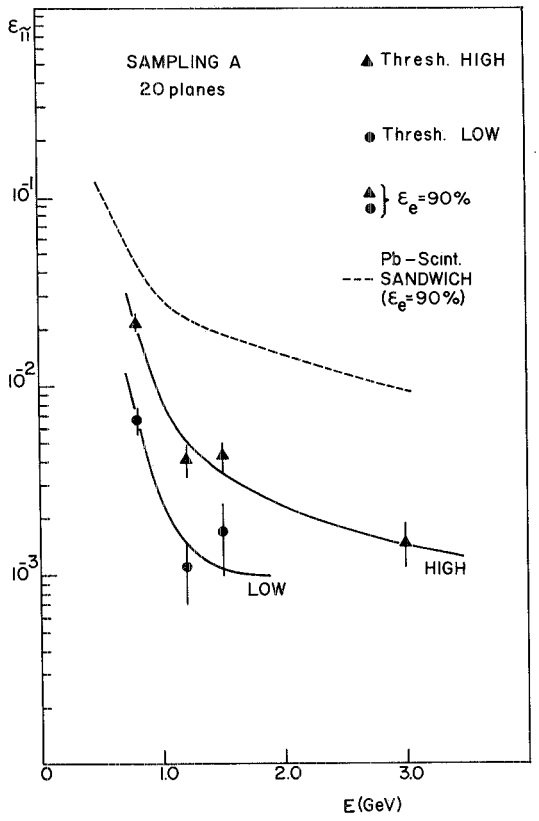

Fig. 8. Pion rejection as function of energy obtained with electronic threshold setting HIGH (upper curve), and LOW (lower curve). As one can see, threshold LOW, i.e. higher multihit M (see text), gives a factor of about 3 better rejection. For the sake of comparison, the dashed upper curve represents the rejection of a lead/scintillator sandwich of comparable thickness (ref. [4]).

simulating calorimeters of different depth. Whilst, in principle, the thicker the calorimeter the better the information available for the pion–electron separation, this is not necessarily true when using the hit multiplicity as the main parameter for operating this separation.

Fig. 10 shows the result of this study. The number of pions surviving, for an overall-all constant 90% electron efficiency, reached a minimum around 12 planes (7.5 r.l.), meaning that a thin calorimeter containing only the electron shower maximum gives the best pion-to-electron separation.

The need for a relatively small number of LST planes (about 12) to have optimum electron discrimination against pions by hit counting was the main result of the test run, which helped when designing the final calorimeter with the minimum amount of electronic channels and the simplest fast decision logic, namely a linear adder.

In order to improve the π/e separation, other more sophisticated criteria have been studied in conjunction with those mentioned above. These new criteria show evidence of the differences existing between the e.m. and hadron showers in the longitudinal, transverse, and asymmetric distribution of the hits. These criteria are briefly described below, as they result from an optimization process.

i. Longitudinal properties

– Early shower development (ESD) [5]. The total number of hits in the first 2.6 r.l. (planes 2–5) is compared with the remaining number of hits.

ii. Transverse properties

The following criteria are based on the fact that an e.m. shower develops a large transverse width in the first radiation lengths (2-3 r.l.), whilst a pion penetrates as a straight track.

– Mean track width ($\langle W \rangle$). This parameter is given by the maximum distance between two hits in one plane, averaged in the first 2 r.l. (planes 2–4).

– Mean track dispersion ($\langle D \rangle$). This parameter results from the sum of the square distance of each hit in one plane with respect to the line of flight of the incoming particle. The average is done on the first 3.7 r.l. (planes 2–7).

– First plane (FP) where a big cluster is found. In the first 2 r.l. (planes 2–4) a track must have at least one cluster of size ≥ 3 to be accepted as an electron.

iii. Asymmetric properties

These criteria are based on the fact that where a pion interacts via a charge-exchange reaction the resulting e.m. shower is not symmetric with respect to the line of flight of the incoming particle.

– Left–right asymmetry (LRA). The total number of hits at the left side with respect to the line of flight of the incoming particle is compared with the corresponding number at the right side in each orthogonal view.

– Containment cone (CC) [6]. This parameter is given by the total number of hits inside a cone of aperture θ centred on the incoming particle. Various values of θ have been tried (6°, 12°, 17°).

To evaluate and compare the relative power, all these criteria have been tested in combinations with the cut on total multiplicity, which is anyway the principal criterion, keeping the global efficiency for electrons constant at 90%. The tests have been done at 800 MeV/c, which is the most critical energy for the e/π separation and the most crucial for the experiment. The results are summarized in table 3. In the third column have been applied using all the hits of the event, whilst in the fourth column only hits clusters of size ≥ 3 have been used.

The final conclusion of all the above studies was that the simplest parameters are also the best ones. The cut in the total number of hits inside clusters of size ≥ 3, coupled with that on the track width parameter $\langle W \rangle$, was finally used to achieve the best pion rejection

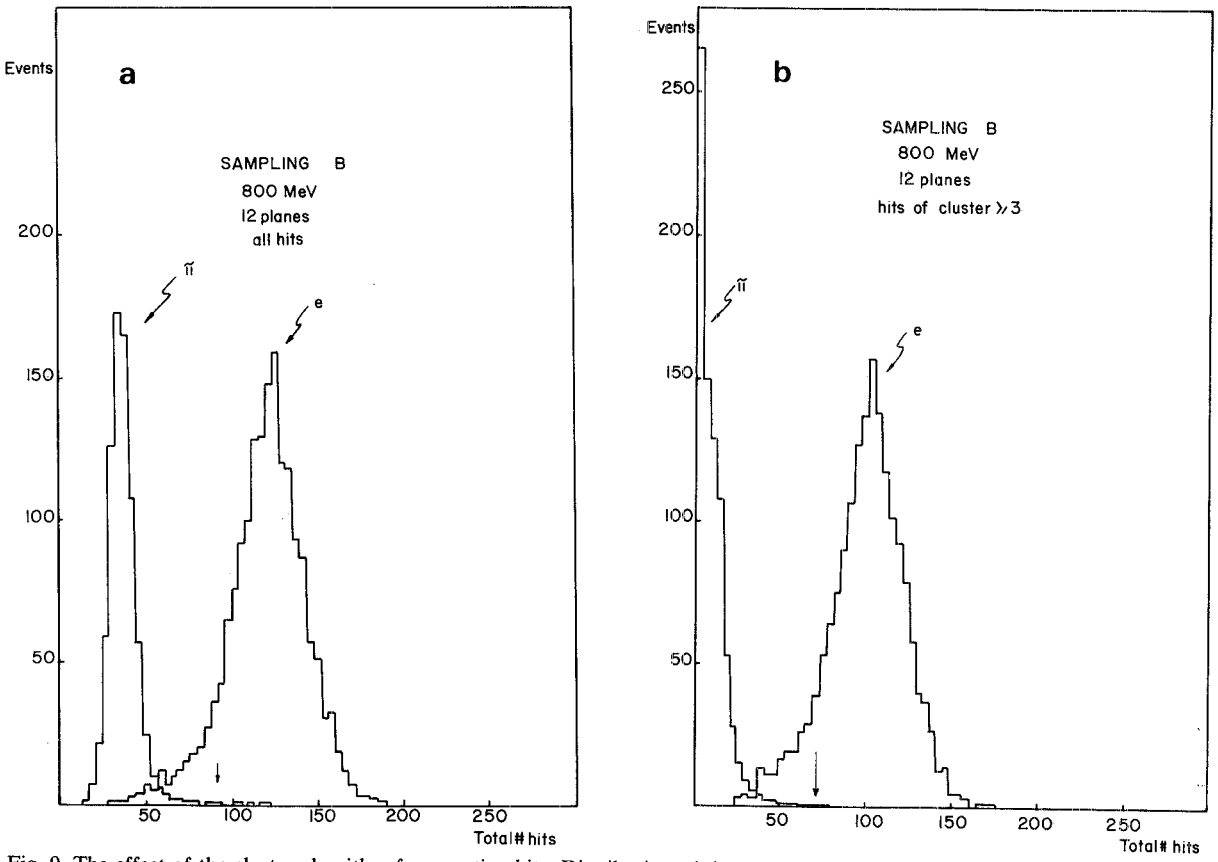

Fig. 9. The effect of the cluster algorithm for counting hits. Distribution of the total number of hits for pions and electrons: (a) the sum of x- and y-strip hits is plotted; (b) the hits of clusters of size ≥ 3 only are counted. The arrows show a cut for 90% electron efficiency.

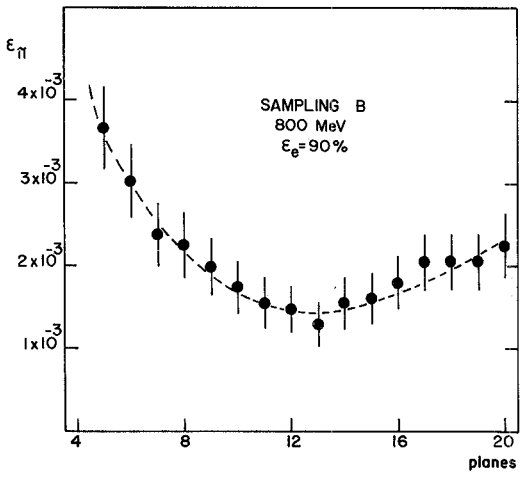

Fig. 10. Pion rejection versus calorimeter depth. The fraction of pion events surviving a cut in the total number of hits counted in clusters of size ≥ 3, which allows 90% electron efficiency, is plotted as a function of the number of LST calorimeter planes used in the analysis. As one can see, there is an optimum rejection of pions for a calorimeter depth of about 12 LST planes.

factor. This factor is plotted in fig. 11 as a function of the electron energy: above 1 GeV the pion rejection reaches the lowest value of $\sim 6 \times 10^{-4}$, almost energy-independent.

If a very high π/e rejection power is needed, the request of 90% electron efficiency is not the best compromise. To find what the best compromise could be, we have studied the ratio between the pion efficiency and the electron efficiency at 800 MeV (see fig. 12). From the curve shown in this figure we can see that the best compromise between the two efficiencies is around 80% for the electron efficiency. Near this value, the ratio reaches a plateau, which means that no substantial gain in π/e rejection power is obtainable.

5. Conclusions

The test performed on this LST electromagnetic calorimeter have shown that this new instrument is particularly suitable for detecting low-energy electrons (around 1 GeV) when the experimental requirement is a very high pion–electron discrimination. In fact, after

Table 3
Pion rejection factor at 800 MeV/c, for a constant 90% electron efficiency, obtained with a cut on the total number of hits combined with various rejection criteria described in the text.

		All hits	Only hits inside clusters of size ≥ 3
Longitudinal development	Early shower development	2.0 ± 0.4‰	1.6 ± 0.3‰
Transverse development	mean track width	1.9 ± 0.4‰	0.9 ± 0.2‰
	mean track dispersion	2.6 ± 0.4‰	2.0 ± 0.4‰
	first plane	1.4 ± 0.3‰	1.4 ± 0.3‰
Asymmetric development	left–right asymmetry	1.6 ± 0.3‰	1.7 ± 0.3‰
	containment cone (6°)	2.8 ± 0.4‰	2.4 ± 0.4‰
	containment cone (12°)	2.7 ± 0.4‰	2.3 ± 0.4‰
	containment cone (17°)	2.6 ± 0.4‰	2.2 ± 0.4‰

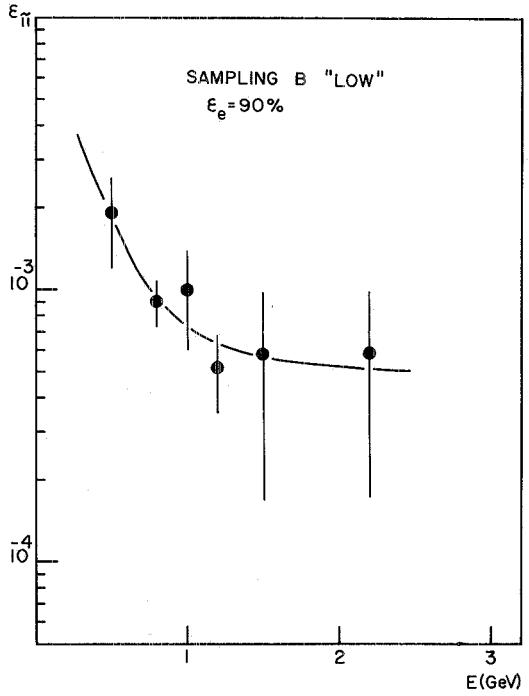

Fig. 11. Ultimate pion rejection power as a function of beam energy for electron detection efficiency of 90%, obtainable applying two optimized cuts in the number of hits and in the track width, and considering only clusters of size ≥ 3.

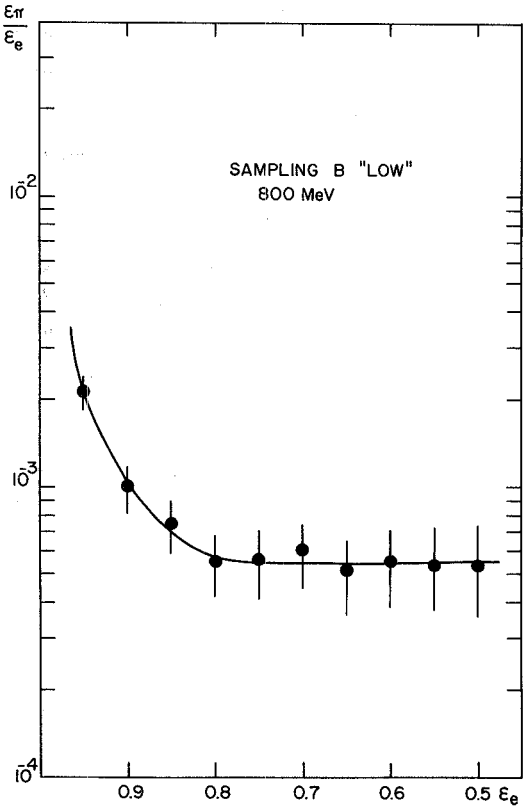

Fig. 12. Ratio between pion efficiency and electron efficiency at 800 MeV electron efficiency. The curve is hand-drawn.

having optimized all the hardware and software parameters, an ultimate pion rejection factor of $\sim 6 \times 10^{-4}$ for energies ≳ 1.2 GeV can be reached with simple off-line analyses. Furthermore, a cut on the total number of hits, such that 90% of 800 MeV energy electrons are accepted, already ensures a 10^{-2} rejection against pions. Such a cut is easy to obtain with fast electronic circuits and can therefore be used in the first stage of a selective trigger experiment.

For a given energy of electrons to be detected, there is an optimum calorimeter depth for which the pion rejection, by cutting on the total number of hits, has a maximum. For 800 MeV electrons the optimum depth was about 12 planes in our calorimeter, corresponding to 7.5 r.l.

Another important characteristic shown by our tests was the rate of particles that can be handled by a calorimeter built using LST planes with cathode-strip readout is much higher than that foreseen in a high-luminosity colliding beam machine such as the CERN ISR.

On the basis of the above results, two electromagnetic calorimeter modules have been built, both with the following characteristics:

i) sensitive area 2.32×2.38 m^2 obtained using standard LST 16-tube modules, 2.5 m long and 1×1 cm^2 cross-section;
ii) total thickness 7.5 r.l. of lead subdivided into 11 layers: a first layer, 5 mm thick, then five layers of 3 mm followed by five layers of 4 mm; each layer of lead was glued to a low-density cellular structure, 5 cm thick, ensuring both mechanical rigidity and a low packing density of about 9 cm per radiation length;
iii) total number of sensitive planes: 12, the first LST plane being in front of the first lead converter; for each plane a bidimensional inductive readout with vertical y-strips (along wires, spacing 1 cm) and horizontal z-strips (across wires, spacing 1.2 cm);
iv) total number of electronic channels: 4992, each of the 12 LST planes consisting of 224 y-strips and 192 z-strips;
v) remote control of high voltages and hardware electronic thresholds on all channels, to monitor the working conditions; linear adders and fast shaping for groups of strip signals, to be used at the fast trigger level; monitoring of gas mixture and gas flow in the LST modules; protection against short circuits and wire faults.

On the basis of the test module results, such an electromagnetic calorimeter is expected to have a very good pion rejection, energy resolution, and linearity, adequate for the purposes of the experiment on the study of heavy flavours at the ISR [7].

We wish to thank dr. Paola dal Piaz for the helpful discussions in preparing this text. We are very grateful to W. Lelli, R. Pilastrini and M. Ventura for assembling and installing the detectors. We wish to thank R. Volta for his contributions to the fast linear electronics, A. Bugatti and S. Tofanelli for their excellent work on the mechanics, and H. Bienkowski for his continuous support in solving problems in connection with the latter. We also thank G. Bonora, V. Biffoni, R. Droghetti and G. Molinari for the skilfull assistance in mounting the LST modules.

References

[1] M. Basile, G. Cara Romeo, L. Cifarelli, A. Contin, G. D'Ali, P. DiCesare, B. Esposito, P. Giusti, T. Massam, R. Nania, F. Palmonari, G. Sartorelli, G. Valenti and A. Zichichi, Nuovo Cimento 63A (1981) 230, Nuovo Cimento 65A (1981) 457 and Nuovo Cimento 67A (1982) 40.
[2] M. Basile, G. Bonvicini, G. Cara Romeo, L. Cifarelli, A. Contin, G. D'Ali, P. DiCesare, B. Esposito, P. Giusti, T. Massam, R. Nania, F. Palmonari, G. Sartorelli, G. Valenti and A. Zichichi, Nuovo Cimento Lett. 31 (1981) 97.
[3] G. Battistoni, E. Iarocci, M.M. Massai, G. Nicoletti and T. Trasatti, Nucl. Instr. and Meth. 164 (1979) 57.
[4] M. Basile, G. Cara Romeo, L. Cifarelli, A. Contin, G. D'Ali, P. Giusti, T. Massam F. Palmonari, G. Sartorelli, G. Valenti and A. Zichichi, Nucl. Instr. and Meth. 163 (1979) 93.
[5] T. Massam, Th. Muller and A. Zichichi, CERN 63-25 (1963).
[6] T. Massam, Th. Muller, M. Schneegans and A. Zichichi, Nuovo Cimento 39 (1965) 464.
[7] M. Basile, G. Bonvicini, G. Cara Romeo, L. Cifarelli, A. Contin, G. D'Ali, P. DiCesare, B. Esposito, M. Esposito, P. Giusti, T. Massam, R. Nania, F. Palmonari, A. Petrosino, F. Rohrbach, V. Rossi, G. Sartorelli, M. Spinetti, G. Susinno, G. Valenti, G. Votano and A. Zichichi, CERN/ISRC/81-27 (1981).